

Electron spin resonance in $\text{EuFe}_{2-x}\text{Co}_x\text{As}_2$ single crystals

J. J. Ying, T. Wu, Q. J. Zheng, Y. He, G. Wu, Q. J. Li, Y. J. Yan, Y. L. Xie, R. H. Liu, X. F. Wang, and X. H. Chen*
*Hefei National Laboratory for Physical Science at Microscale and Department of Physics, University of Science and Technology of China,
 Hefei, Anhui 230026, People's Republic of China*

(Received 31 July 2009; revised manuscript received 23 September 2009; published 12 February 2010)

The temperature dependence of electron spin resonance (ESR) was studied in $\text{EuFe}_{2-x}\text{Co}_x\text{As}_2$ system. The ESR spectrum of all the samples indicates that the linewidth strongly depends on the temperature. Moreover, the linewidth shows the Korringa behavior, indicating an exchange coupling between the conduction electrons and the Eu^{2+} ions. The linewidth, g factor and the integrate ESR intensity show anomalies at the temperature of the spin-density-wave (SDW) ordering. The linewidth below the SDW transition does not rely on the temperature. This gives the evidence for the gap opening at the T_{SDW} . The slope of the linewidth is closely associated to T_{SDW} and T_c . Such exotic behavior should be related to the nesting of the Fermi surface.

DOI: 10.1103/PhysRevB.81.052503

PACS number(s): 31.30.Gs, 71.38.-k, 75.30.-m

The discovery of Fe-based high- T_c superconductor provides a family of materials to explore the mechanism of high- T_c superconductivity besides high- T_c cuprates superconductor.¹⁻⁵ Ternary iron arsenides AFe_2As_2 ($A = \text{Sr, Ca, Ba, Eu}$) is one of parent compounds with ThCr_2Si_2 -type structure. In analogy with LnFeAsO ($\text{Ln} = \text{La-Gd}$), AFe_2As_2 undergoes a structural phase transition with spin-density-wave (SDW) ordering, evidenced by the anomalies in resistivity, susceptibility, and specific heat. With introducing carrier, the ground state of FeAs compounds evolves from SDW state to superconducting (SC) state.

EuFe_2As_2 is a unique member in the ternary iron arsenide family due to the large local moment of Eu^{2+} , which orders antiferromagnetically below 20 K.^{6,7} Except for this antiferromagnetic transition, the physical properties of EuFe_2As_2 are found to be quite similar with those of its isostructural compounds AFe_2As_2 . Wu *et al.*⁷ have given the evidence for a coupling between magnetism of Eu^{2+} ions and SDW ordering in FeAs layer. Study on the interaction between the conduction electrons of FeAs layer and localized spins of Eu^{2+} layer gives significant information about the properties of FeAs layer. The electron spin resonance (ESR) spectra in metals are very effective to study the interaction with the conduction electrons and local moments, which has been widely applied in high- T_c cuprates.^{8,9}

In this Brief Report, we systematically studied the ESR spectra of the single crystals $\text{EuFe}_{2-x}\text{Co}_x\text{As}_2$ with different x . The g factor, the linewidth, and the integrated ESR intensity show the anomaly at T_{SDW} . The linewidth of the samples shows the Korringa behavior above T_{SDW} , indicating an exchange coupling between the conduction electrons and spin of the Eu^{2+} ions. The fact that linewidth becomes temperature independence below T_{SDW} gives the evidence for the gap opening at T_{SDW} . The slope of the linewidth shows interesting behavior with Co doping and is closely related to the characteristic temperature: T_{SDW} and T_c .

High-quality single crystals with nominal composition $\text{EuFe}_{2-x}\text{Co}_x\text{As}_2$ ($x=0, 0.067, 0.1, 0.2, 0.25, 0.275, 0.285, 0.35, 0.4, 0.45, \text{ and } 0.5$) were grown by self-flux method as described elsewhere.¹⁰ Many shining platelike $\text{EuFe}_{2-x}\text{Co}_x\text{As}_2$ crystals were obtained. The ESR measurements of the single crystals were performed using a Bruker ER-200D-SRC spectrometer, operating at X-band frequen-

cies (9.07 GHz) and between 110 and 300 K. The resistance was measured by an ac resistance bridge (LR-700, Linear Research). It should be addressed that all results discussed here are well reproducible. The measurements were carried with the magnetic field applied along c axis of single crystals.

Figure 1 shows temperature dependence of in-plane resistivity for single crystals $\text{EuFe}_{2-x}\text{Co}_x\text{As}_2$ with $x=0, 0.067, 0.1, 0.2, 0.25, 0.275, 0.285, 0.35, 0.4, 0.45, \text{ and } 0.5$. For parent compound EuFe_2As_2 , the resistivity shows a steep increase around 188 K, and reaches its maximum value around 180 K. It is associated with SDW and structure transition. The kink at about 20 K is related to antiferromagnetic ordering of Eu^{2+} moments. With Co doping, the SDW transition is gradually suppressed. For the crystal with $x=0.25$, the SDW transition was completely suppressed and superconducting transition shows up at $T_c \sim 22$ K, but the resistance could not reach zero due to the antiferromagnetic ordering of Eu^{2+} ions. This issue is studied in separated work.¹¹ For the optimally doped crystal with $x=0.285$, T_c reaches 24.5 K. For $x=0.35, x=0.4, \text{ and } x=0.45$ samples, T_c decreases to 21, 20, and 12 K, respectively, while neither the SDW transition nor the superconductivity is observed for the crystal with $x=0.5$.

Figures 2(a) and 2(b) show temperature dependence of ESR spectra for the parent compound EuFe_2As_2 and the representative sample $\text{EuFe}_{1.933}\text{Co}_{0.067}\text{As}_2$ in the temperature

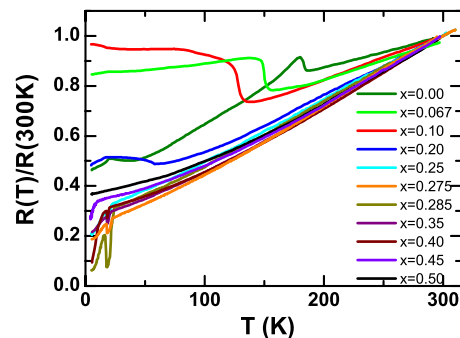


FIG. 1. (Color online) Temperature dependence of in-plane resistivity for the single crystals $\text{EuFe}_{2-x}\text{Co}_x\text{As}_2$ with $x=0, 0.067, 0.1, 0.2, 0.25, 0.275, 0.285, 0.35, 0.4, 0.45, \text{ and } 0.5$.

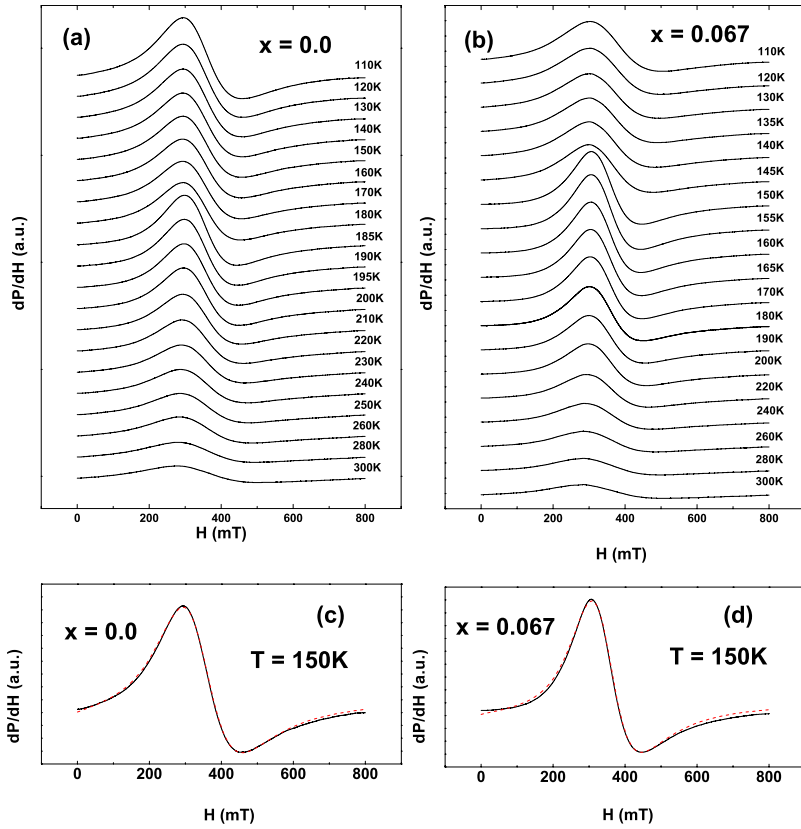


FIG. 2. (Color online) Temperature dependence of ESR spectrum for (a) $x=0.0$ and (b) $x=0.067$. (c) and (d) show the original data (black line) and the fit results (red dashed line) at 150 K for $x=0.0$ and $x=0.067$, respectively.

ranging from 110 to 300 K, respectively. A well-defined paramagnetic signal was observed in the whole temperature range. We ascribe the signal to the Eu ions because only weak signal can be detected in the BaFe_2As_2 single crystal. All the spectrum can be well fitted by the Dysonian shape,¹² given by $\frac{dP}{dH} \propto \frac{d}{dH} \left[\frac{\Delta H + \alpha(H - H_{res})}{(H - H_{res})^2 + \Delta H^2} + \frac{\Delta H + \alpha(H + H_{res})}{(H + H_{res})^2 + \Delta H^2} \right]$. Here H_{res} is the resonance field, ΔH is the half linewidth at half of the maximum absorption, and α is the dispersion-to-absorption ratio used as fitting parameter. Figures 2(c) and 2(d) show the typical fitting results at 150 K. The intensity of the spectra is obviously suppressed with increasing temperature. The spec-

trum abruptly becomes narrow and the intensity is enhanced around T_{SDW} . The spectrum broadens and the intensity decreases with further increasing temperature. The detailed analysis on the spectrum is discussed later on. In other Co-doped compounds, the similar signal has also been observed.

We analyzed temperature dependence of ESR spectrum for $x=0.0$ and $x=0.067$ samples. For the two samples, the SDW transition temperatures are 188 and 158 K determined from the resistivity as shown in Fig. 1, respectively. Figure 3(a) illustrates the linewidth (ΔH) and the g factor as a function of temperature for the $x=0.0$ sample. ΔH is achieved

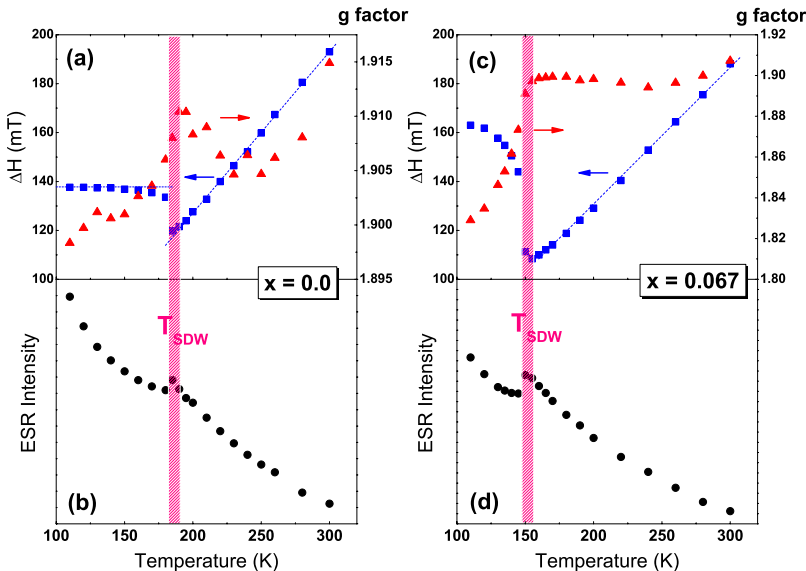


FIG. 3. (Color online) Temperature dependence of g factor and ΔH_{pp} for the crystal with (a) $x=0.0$ and (c) $x=0.067$. Temperature dependence of ESR intensity for the crystal with (b) $x=0.0$ and (d) $x=0.067$. The blue dashed line shows the fitting with linear behavior.

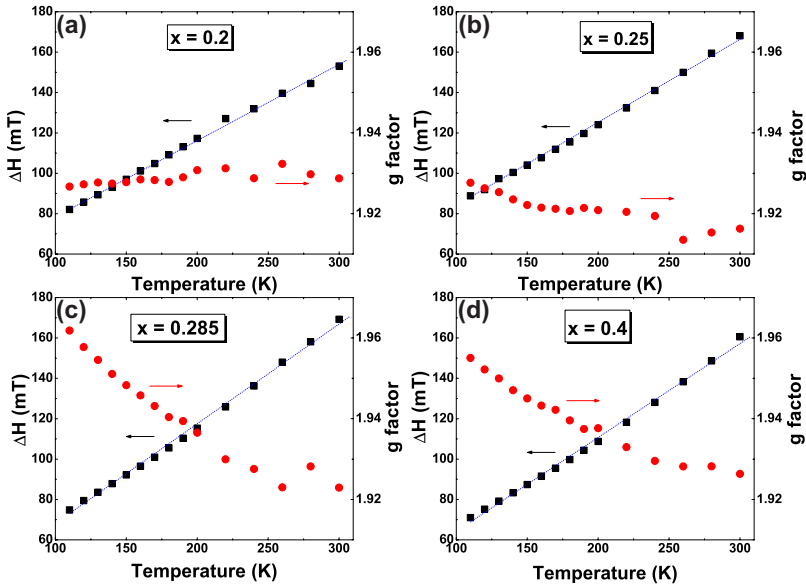


FIG. 4. (Color online) Temperature dependence of g factor and ΔH_{pp} for the crystal with (a) $x=0.20$; (b) $x=0.25$; (c) $x=0.285$; and (d) $x=0.4$. The blue dotted line shows a linear fitting.

from the fitting parameter of temperature-dependent ESR spectrum. The linewidth decreases linearly with decreasing temperature above the SDW transition temperature. Such behavior is also observed in the isostructural EuCu_2Si_2 single crystals.¹³ ΔH shows a sudden jump and begins to deviate from the linear trend at T_{SDW} . At the temperature below T_{SDW} , ΔH becomes temperature independent. The resonance field (H_{res}) to calculate the effective g factor is achieved from the fitting parameter to the ESR spectrum. The effective g factor is calculated with the following formula: $g = \frac{h\nu}{\mu_B H_{\text{res}}}$. For the parent compound, a kink is observed at T_{SDW} . The g factor gradually decreases below T_{SDW} . The ESR intensity of the parent compound obtained by numerical integration is illustrated in Fig. 3(b). It is found that the ESR intensity follows Curie-Weiss formula at high temperature with a kink at T_{SDW} . The anomaly of the ESR intensity below T_{SDW} should be ascribed to the skin effect.¹⁴ Figures 3(c) and 3(d) show temperature dependence of the linewidth, the g factor and the ESR intensity for the $x=0.067$ sample. Their behavior is similar to that of the parent compounds and an anomaly is observed at T_{SDW} . The ΔH also shows the linear behavior above T_{SDW} . All these results confirm the interaction between the local moments of the Eu^{2+} and the conduction electrons in the FeAs layers. Comparing the $x=0.067$ sample with the parent compound, we find the jump of the linewidth at T_{SDW} is larger than the parent compound, and the decrement of the g factor below T_{SDW} is much larger than the parent compound.

The linewidth and the g factors for the four typical Co-doped crystals with $x=0.20$, 0.25 , 0.285 , and 0.40 are shown in Fig. 4. As shown in Fig. 1, the T_{SDW} was suppressed down to 58 K for the $x=0.20$ crystal. The $x=0.25$ crystal with $T_c=22$ K is in the underdoped region. The $x=0.285$ sample is at the optimal doping level and its $T_c=24.5$ K, nearly the same as the highest $T_c=25$ K in Co-doped BaFe_2As_2 .¹⁵ The $x=0.40$ sample with $T_c=20$ K is in the overdoped region. The linewidth of all the samples follows the temperature-linear dependence. This phenomenon is consistent with the behavior observed in the $x=0$ and 0.067 samples above T_{SDW}

as shown in Figs. 3(a) and 3(c). The g factor nearly keeps constant for the samples of the low Co-doped samples. For the heavily doped samples, the g factor increases slightly with decreasing temperature. No anomaly is found in these four compounds.

To systematically investigate the effect of Co doping in $\text{EuFe}_{2-x}\text{Co}_x\text{As}_2$, the ESR spectrum of the other samples with different doping level were measured. It is found that the temperature-dependent linewidth for all the samples shows the same behavior. The linear temperature-dependent linewidth is observed in all the samples above T_{SDW} . Figure 5 illustrates the slope of the linewidth, T_{SDW} and T_c as a function of Co doping. It is striking that the slope of the linewidth shows a close relation with the T_{SDW} and T_c . As shown in Fig. 5, the SDW ordering is gradually suppressed and T_{SDW} decreases with increasing Co doping. It is intriguing that the slope of the linewidth shows the same behavior as that of T_{SDW} and the slope of the linewidth decreases with increasing Co doping in the underdoped region. With further in-

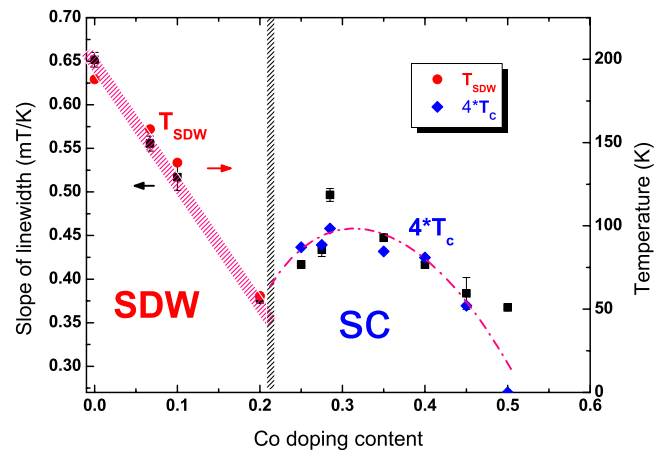


FIG. 5. (Color online) The slope of peak-to-peak linewidth as a function of the Co-doping content. The black squares denote the slope of linewidth and the red circles present the SDW transition temperature and the blue diamonds present the 4^*T_c .

creasing Co doping, the superconductivity emerges and the slope of linewidth begins to increase. In the superconducting region, the slope of linewidth shows the same behavior as T_c . Both the slope of linewidth and T_c exhibit a dome-like behavior with increasing the Co doping. The evolution of the slope of linewidth with Co doping is qualitatively consistent with that of T_{SDW} and T_c .

Spin relaxation of magnetic moments in conventional metals mainly depends on the relaxation times between local moments and itinerated electrons, and spin-lattice relaxation time for itinerated electrons and spin-lattice relaxation time for local moments.^{16–18} The linewidth is a measurement of the relaxation for the spin system. The exchange interaction between local moments and conduction electrons results in a temperature-linear contribution to the total ESR linewidth.⁸ It follows the Korringa behavior $\Delta H = \Delta H_K + \Delta H_{res}$. ΔH_{res} is the residual linewidth and ΔH_K is the Korringa broadening given by $\Delta H_K = \frac{\pi K_B T}{g \mu_B} [J_{Ss} \rho(\epsilon_F)]^2$. Here μ_B is the Bohr magneton, K_B is the Boltzmann constant, J_{Ss} is the exchange interaction between the local moments (S) and the spin of the conduction carriers (s), $\rho(\epsilon_F)$ is the density of states at Fermi surface. The local moment should come mainly from the Eu atom in $\text{EuFe}_{2-x}\text{Co}_x\text{As}_2$ system. The linear linewidth above T_{SDW} for all the samples follows the Korringa law. When SDW transition happens, the linear linewidth behavior is destroyed. The “free-ion” g factor for Eu is normally given as 1.993 in an insulating host.¹⁷ The g factor of Eu ions in these materials is smaller than 1.993 in the whole temperature range. The g factor is almost constant except for high Co-doped samples above T_{SDW} and a kink shows up at T_{SDW} . Such behavior is different from the LaOFeAs system in which ferromagnetic fluctuation from local moment of Fe ions was observed.¹⁸ Such difference arises from the behavior dominated by Eu^{2+} in $\text{EuFe}_{2-x}\text{Co}_x\text{As}_2$ system due to the large local moments of Eu^{2+} . The ESR integral intensity, which is proportional to the spin susceptibility, also shows an anomaly at T_{SDW} . In the parent compound, the linewidth becomes temperature independent below T_{SDW} so that the linewidth slope is zero. If it is assumed that the Korringa law is applicable below T_{SDW} , the $\rho(\epsilon_F)$ should be zero. This result suggests that the density of state losses at the Fermi surface and a gap opens at T_{SDW} . Such behavior of linewidth has

been observed in the Kondo insulator CeNiSn .¹⁹ The slope of linewidth exhibits an interesting behavior with Co doping, and it shows a close relation with T_{SDW} and T_c . Because the J_{Ss} between the Eu^{2+} and the conduction electrons does not change with Co doping, the difference of the slope should come from the density of state at Fermi surface. Recently, Terashima *et al.*²⁰ observed isotropic SC gaps which depend on the nesting conditions of Fermi surface. The superconductivity is related to the Fermi-surface topology.²¹ The Fermi-surface nesting may play an important role in the superconductivity and the nesting of Fermi surface has a strong effect on the slope of the linewidth. There are two possible explanation for the SDW ordering. One possible explanation is that the Fermi surface is perfectly nesting for the parent compounds, resulting in SDW ordering. With Co doping, the Fermi-surface nesting is gradually destroyed, so that the slope decreases with Co doping in the SDW region. While in the SC region, the Fermi-surface nesting condition is changed, and the superconductivity is closely related to the Fermi-surface nesting based on the study by Terashima *et al.*²⁰ The behavior of the slope associated with the T_{SDW} and T_c could be related to the complicated nesting of Fermi surface.

In conclusion, we studied the temperature dependence of ESR spectrum for single crystals $\text{EuFe}_{2-x}\text{Co}_x\text{As}_2$ system. Strong temperature dependence of the g factor and ΔH_{pp} are observed in all the samples. The linewidth, the g factor, and the ESR intensity all show anomalies at T_{SDW} . The linewidth for all the samples above T_{SDW} shows the Korringa behavior. These results indicate the exchange interaction between the local moments of Eu^{2+} and the conduction electrons in FeAs layers. A gap opening at T_{SDW} is evidenced by the fact that the linewidth does not change below T_{SDW} . The slope of the linewidth is strongly dependent on the Co-doping content and is closely associated with T_{SDW} and T_c . Such behavior maybe related to the complicated Fermi-surface nesting.

This work is supported by the Nature Science Foundation of China and by the Ministry of Science and Technology of China (973 Project No. 2006CB601001) and by National Basic Research Program of China (Grant No. 2006CB922005).

*Corresponding author; chenxh@ustc.edu.cn

¹Y. Kamihara, T. Watanabe, M. Hirano, and H. Hosono, *J. Am. Chem. Soc.* **130**, 3296 (2008).

²X. H. Chen *et al.*, *Nature (London)* **453**, 761 (2008).

³G. F. Chen *et al.*, *Phys. Rev. Lett.* **100**, 247002 (2008).

⁴Z. A. Ren *et al.*, *EPL* **83**, 17002 (2008).

⁵M. Rotter, M. Tegel, and D. Johrendt, *Phys. Rev. Lett.* **101**, 107006 (2008).

⁶Z. Ren *et al.*, *Phys. Rev. B* **78**, 052501 (2008).

⁷T. Wu *et al.*, *J. Magn. Magn. Mater.* **321**, 3870 (2009).

⁸D. Shaltiel, C. Noble, J. Pilbrow, D. Hutton, and E. Walker, *Phys. Rev. B* **53**, 12430 (1996).

⁹V. Kataev, Yu. Greznev, G. Teitel'baum, M. Breuer, and N. Knauf, *Phys. Rev. B* **48**, 13042 (1993).

¹⁰X. F. Wang *et al.*, *Phys. Rev. Lett.* **102**, 117005 (2009).

¹¹Q. J. Zheng *et al.*, arXiv:0907.5547 (unpublished).

¹²V. A. Ivashin *et al.*, *Phys. Rev. B* **61**, 6213 (2000).

¹³C. D. Cao *et al.*, *Phys. Rev. B* **78**, 064409 (2008).

¹⁴E. Dengler *et al.*, arXiv:0909.2054 (unpublished).

¹⁵X. F. Wang *et al.*, *New J. Phys.* **11**, 045003 (2009).

¹⁶R. H. Taylor, *Adv. Phys.* **24**, 681 (1975).

¹⁷S. E. Barnes, *Adv. Phys.* **30**, 801 (1981).

¹⁸T. Wu *et al.*, *Phys. Rev. B* **79**, 115121 (2009).

¹⁹S. Mair, H.-A. Krug von Nidda, M. Lohmann, and A. Loidl, *Phys. Rev. B* **60**, 16409 (1999).

²⁰K. Terashima *et al.*, *Proc. Natl. Acad. Sci. U.S.A.* **106**, 7330 (2009).

²¹Y. Sekiba *et al.*, *New J. Phys.* **11**, 025020 (2009).